Modulation of Eastern North Pacific Hurricanes by the Madden–Julian Oscillation

ERIC D. MALONEY AND DENNIS L. HARTMANN

Department of Atmospheric Sciences, University of Washington, Seattle, Washington

(Manuscript received 8 February 1999, in final form 12 May 1999)

ABSTRACT

Hurricane and tropical storm statistics verify the modulation of eastern Pacific tropical systems by the Madden–Julian oscillation (MJO) as hypothesized by Maloney and Hartmann. Over twice as many named tropical systems (hurricanes and tropical storms) accompany equatorial 850-mb westerly anomalies than accompany equatorial easterly anomalies, and the systems that do exist are stronger. Hurricanes are over four times more numerous during westerly phases of the MJO than during easterly phases.

The current study constructs a composite life cycle of the MJO during May–November 1979–95 using an index based on the 850-mb equatorial zonal wind. Equatorial Kelvin waves propagating eastward from convective regions of the western Pacific Ocean alter dynamical conditions over the eastern Pacific Ocean. Westerly (easterly) equatorial 850-mb wind anomalies are accompanied by enhanced (suppressed) convection over the eastern Pacific hurricane region. Convection locally amplifies the wind anomalies over the eastern Pacific.

Cyclonic horizontal shear of the low-level zonal wind and low vertical wind shear support tropical cyclogenesis. Periods of equatorial 850-mb westerly wind anomalies associated with the MJO are accompanied by cyclonic low-level relative vorticity anomalies and near-zero vertical wind shear over the eastern Pacific hurricane region. Easterly periods are accompanied by anticyclonic vorticity anomalies and less-favorable vertical wind shear. The vorticity anomalies are associated with variations in the meridional shear of the zonal wind.

1. Introduction

The Madden–Julian oscillation (MJO) is a dominant mode of variability in the tropical atmosphere with characteristic periods of 30–60 days. The MJO has a baroclinic mixed Kelvin and Rossby wave structure in the Indian and western Pacific Oceans, where the equatorial wave is strongly coupled to convection. Rossby wave structure dominates to the west of convection. Propagation in convective regions is eastward at roughly 5 m s^{-1}. Kelvin waves propagate eastward out of the convective regions at phase speeds of 10–12 m s^{-1}. Anomalous winds at 850 mb can extend to the coast of South America where the Andes Mountains appear to block further propagation. Anomalies at 200 mb can travel the entire circuit of the equatorial belt. See Madden and Julian (1994) and Hendon and Salby (1994) for thorough reviews.

Maloney and Hartmann (1998, hereinafter referred to as MH98) composited the MJO based on an index of the first two empirical orthogonal functions (EOFs) of the bandpass-filtered equatorial 850-mb zonal wind. The two EOFs are dominated by zonal winds in the western Pacific and Indian Oceans. During certain phases of the MJO, a modulation of convective activity occurs over the eastern Pacific Ocean near Mexico and Central America, especially during Northern Hemisphere summer. In the eastern Pacific during the composite life cycle, westerly 850-mb wind anomalies accompany periods of intensified convection and easterly anomalies accompany suppressed convection. Equatorial wind anomalies of the opposite sign occur at upper levels. These wind variations are in phase with eastward-propagating MJO Kelvin waves from the western Pacific. A local amplification of the wind anomalies occurs over the eastern Pacific because of enhanced convection. Some of the strongest wind anomalies in the composite life cycle occur in the eastern Pacific during these times. Cyclonic (anticyclonic) meridional shear anomalies of the low-level zonal wind occur between the equator and 30°N during enhanced (suppressed) periods of convection. MH98 speculated that the MJO could play a role in regulating tropical cyclone activity in the eastern north Pacific Ocean through variations in this meridional shear. Previous work about these connections has been sparse. Although not mentioned in their work, the MJO composites of Hendon and Salby (1994) hint at a similar modulation. Molinari et al. (1997) suggest that MJO wave disturbances and associated shear variations may create periods of instability over the Caribbean Sea and the eastern Pacific through a reversal of the meridional

Corresponding author address: Mr. Eric Maloney, Department of Atmospheric Sciences, University of Washington, Box 351640, Seattle, WA 98195-1640.
E-mail: maloney@atmos.washington.edu

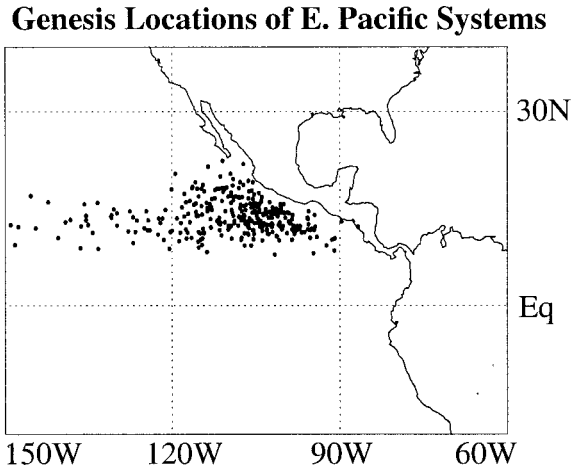

FIG. 1. Genesis locations of eastern Pacific Ocean tropical systems attaining wind speeds of tropical storm force (34 kt) or greater during May–Nov 1979–95.

potential vorticity gradient. Cyclogenesis would be favored during these times. Modulation of eastern Pacific hurricanes by the MJO can help explain the observation by Gray (1979) that tropical cyclones tend to cluster in time.

MJO wave anomalies propagating into the eastern Pacific from the west are locally amplified by enhanced convection. Westerly wind anomalies over the eastern Pacific can foster increased convection through anomalous cyclonic low-level shear on the northern flank of the maximum winds and associated low-level convergence. Forced Rossby waves can then intensify the atmospheric circulation, increasing the low-level westerly winds. Inflow into convection over Central America, Mexico, and the western Caribbean Sea can also strengthen the circulation over the eastern Pacific. Topographic enhancement of convection over land areas may be a factor.

Figure 1 shows the genesis locations of eastern Pacific systems attaining at least tropical storm strength (34 kt) for the years 1979–95. The genesis location denotes where the tropical cyclone first achieved a sustained wind speed of 34 kt. The figure was derived from National Oceanic and Atmospheric Administration (NOAA) National Weather Service (NWS) Tropical Prediction Center storm track information (Brown and Leftwich 1982). We will analyze tropical cyclone activity to the east of 140°W, the region traditionally defined as the eastern North Pacific hurricane basin and the region of local amplification of the MJO signal in the composites of MH98. Tropical cyclone formation usually occurs over climatologically warm waters near Mexico and Central America during May–November. Typical movement is toward the west-northwest. An average of 16.4 named systems (tropical storms, wind $\geq$ 34 kt; hurricanes, wind $\geq$ 64 kt) occur in the eastern Pacific basin each year. The number of hurricanes averages 9.4. By comparison, the Atlantic basin averages only 9.8 named storms per year and 5.8 hurricanes.

The three most important environmental dynamical factors in tropical cyclone genesis are low-level relative vorticity, vertical wind shear, and the Coriolis parameter (Gray 1979; McBride and Zehr 1981; Davidson et al. 1990). Tropical cyclogenesis is favored in environments with highly cyclonic low-level relative vorticity and low vertical wind shear. Development occurs away from the equator where the Coriolis parameter is sufficiently large. Additional environmental factors that may be of some importance are upper-level anticyclonic vorticity and low-level convergence (McBride and Zehr 1981; Molinari and Vollaro 1989; Davidson et al. 1990; Zehr 1992). The current study will concentrate on low-level vorticity and vertical shear, with a brief mention of upper-level vorticity processes. Although low-level convergence will not be emphasized in this study, the composites of MH98 showed that periods of enhanced (suppressed) convection over the eastern Pacific were accompanied by surface convergence (divergence), as would be expected.

Cyclonic shear of the zonal wind may cause a reversal of the potential vorticity gradient to the north of the strongest shear, a condition favorable for instability (Charney and Stern 1962; Nitta and Yanai 1969; Holton 1992; Molinari et al. 1997), although clearly latent heat release is critical to tropical cyclone development. Regions of low-level cyclonic shear also produce low-level convergence through coupling with the boundary layer. Westerly wind bursts in the western Pacific Ocean associated with the MJO create cyclonic shear zones to the north and south of the equator that frequently initiate tropical cyclone formation (Liebmann et al. 1994; Nieto Ferreira et al. 1996). Tropical cyclones in the western Pacific tend to cluster temporally around periods of barotropic instability on the poleward flanks of these shear zones (Gray 1979; Schubert et al. 1991; Nieto Ferreira and Schubert 1997). Latent heat release and vortex spinup can in turn accelerate the low-level westerly winds near the equator, creating a positive feedback mechanism (Nitta 1989; Nieto Ferreira et al. 1996). Hartmann et al. (1992) document a similar modulation of typhoon activity in the western Pacific in association with a 20–25-day oscillation that occurs during the typhoon season. Their composites suggest a connection between equatorial low-level winds, surface pressure, and typhoon occurrence. Low-level westerly wind perturbations associated with the MJO propagating into the eastern Pacific Ocean may foster similar interactions there.

High vertical wind shear causes vorticity centers at upper and lower levels to be displaced in the horizontal. Vertical tilting of the vortex circulation requires an increased midlevel temperature perturbation for a balanced mass field (DeMaria 1996). This increased midlevel temperature perturbation tends to inhibit convection, suppressing growth of the vortex. The favored position for tropical cyclone formation is along a zero line

in the vertical shear of the zonal wind between regions of high positive vertical shear to the north and high negative vertical shear to the south (Gray 1968; Elsberry et al. 1988). Positive shear is defined as upper-level winds being more westerly than lower-level winds.

This paper examines the dynamical forcing associated with MJO Kelvin wave propagation into the eastern Pacific and its effect on tropical cyclones. A composite lifecycle of the MJO is constructed for May–November using the method of MH98. Dynamical factors present during both suppressed and active phases of convection in the eastern Pacific Ocean will be discussed. Records of eastern Pacific tropical cyclones will be used to verify that the MJO modulates hurricane activity in this region. These results suggest that the MJO modulates hurricane activity by creating favorable conditions for development or suppression of tropical cyclones in the eastern Pacific. Section 2 presents the data and compositing technique. Section 3 displays tropical circulations associated with the MJO in a global context. Section 4 examines eastern Pacific 200- and 850-mb wind, precipitation, and vorticity anomalies as well as vertical shear of the zonal wind for two extreme phases of the MJO. Section 5 uses hurricane records to quantify hurricane activity over an MJO life cycle. Conclusions are presented in section 6.

2. Data and compositing technique

a. Data

The National Centers for Environmental Prediction–National Center for Atmospheric Research (NCEP–NCAR) gridded reanalysis data (2.5° × 2.5°) in pentad format were used for winds at 200 and 850 mb for the years 1979–1995 (Kalnay et al. 1996). Microwave Sounding Unit (MSU) gridded pentad precipitation data (2.5° × 2.5°) were available during this same period (Spencer 1993). This precipitation dataset is only valid over ocean areas, which is acceptable within the scope of the current study. More detail concerning these datasets can be found in MH98. Hurricane and tropical storm tracking data for the northeastern Pacific Ocean (east of 140°W) were obtained from the NOAA/NWS/Tropical Prediction Center (Brown and Leftwich 1982). The dataset documents hurricanes and tropical storms back to 1949. Storm strength and position were recorded four times daily.

b. Compositing technique

The compositing technique described in detail in MH98 is reviewed briefly here. The index used for compositing is based on the 20–80-day bandpass-filtered 850-mb zonal wind averaged from 5°N to 5°S at every longitude. EOF analysis on the entire 17-yr time series (1979–95) yields two prominent EOFs, the first explaining 32% of the variance and the second 22%. They

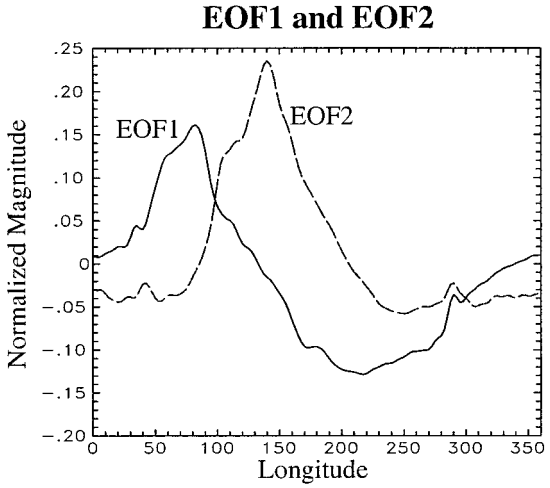

FIG. 2. EOF1 (solid) and EOF2 (dashed) of the 850-mb zonal wind as a function of longitude. Data during 1979–95 in all seasons are used. Magnitudes are normalized.

are shown to be significantly different from the other EOFs by using the criterion developed by North et al. (1982). Principal components (PCs) were derived by projecting the first two EOFs onto the original filtered zonal wind time series. Figure 2 displays the structure of the first two EOFs. Note that the amplitudes of these EOFs peak over the Indian and western Pacific Oceans, but considerable amplitude extends into the eastern Pacific, especially for EOF1. A simultaneous correlation of −0.74 exists between the PC of EOF1 and the 20–80-day bandpass-filtered 850-mb equatorial zonal wind time series at 110°W during May–November. This correlation is significant at the 99% level. The zonal wind time series at 110°W also has a highly significant correlation (0.42) with the PC of EOF2 at a lag of 15 days (110°W time series lags PC time series).

The amplitude of EOF 2 peaks an average of 10–15 days later than that of EOF 1. Thus, EOFs 1 and 2 appear to form a propagating signal in the zonal wind. An index was constructed in the following manner, where t is the time in pentads:

$$\text{Index}(t) = \text{PC1}(t) + [\text{PC2}(t+2) + \text{PC2}(t+3)]/2. \quad (1)$$

The index is a linear combination of PCs 1 and 2 with contributions from PC 2 reflecting that it peaks an average of 2–3 pentads after PC 1. Results were rather insensitive to reasonable variations in the definition of this index. Since the index tends to oscillate sinusoidally, assignment of phases is relatively straightforward. Key events are chosen by selecting periods in which the peak amplitude of the index is greater than one standard deviation from zero. Phase 5 is assigned to the time in each event with maximum positive amplitude. Phases 1 and 9 are assigned to the times in each event with largest negative amplitude before and after phase 5, respectively. Phases 3 and 7 are assigned to the zero crossing points, and the remaining phases are placed equi-

distant between phases 1, 3, 5, 7, and 9. Once the timing of all phases of each event is determined, the events are averaged to produce a composite event. Consecutive phases of the composite event are, on average, 5 days apart.

During the eastern Pacific hurricane season of May–November, 58 events were isolated. Phases 2 and 6 are the periods of strongest westerly and easterly 850-mb zonal wind anomalies in the eastern Pacific, respectively, and they are also the times of greatest and least convection and precipitation in the composite.The most active period of the hurricane season according to the NOAA/NWS/Tropical Prediction Center is June–September. Phases 2 and 6 occur with about equal frequency throughout the June–September period, so the differences between these two phases that we observe are not the result of seasonal biases in the sampling. The same is true for the expanded period of May–November.

One point must be mentioned here. Previous studies have shown that the MJO signal has minimum amplitude during the Northern Hemisphere summer season (Salby and Hendon 1994; Madden and Julian 1994). In fact, the fewest events in our composites occur during July. However, a significant number of events still occur within the hurricane season and in the most intense June–September period. About 50% of the June–September time series and about 60% of the May–November time series during 1979–95 are spanned by significant MJO events as defined by our index. We do not claim that all eastern Pacific hurricanes are affected by the Madden–Julian oscillation. Instead, we claim that significant MJO events can modulate tropical cyclone activity over the eastern Pacific Ocean through local enhancement of eastward-propagating wind anomalies associated with Kelvin wave dynamics.

3. Global life cycle composites

Figure 3 details phases 2, 4, 6, and 8 of the MJO in a global context. The phases are determined from the 850-mb zonal wind index (1). Winds at 850-mb bandpass filtered to 20–80 days and MSU precipitation anomalies are plotted. Precipitation anomalies are constructed by removing the annual cycle. The composites include events from May through November, corresponding to the eastern Pacific Ocean hurricane season.

Growing precipitation anomalies in the Indian Ocean peak at phase 4 and then shift into the western Pacific at phase 6. This convection shifts slightly eastward and weakens during phase 8. Easterly wind anomalies form near and to the east of Indian Ocean convection during phase 2, propagate eastward, and then peak over the eastern Pacific Ocean at phase 6. These anomalous easterlies coincide with suppression of convection near the Central American and Mexican coasts. Anomalies at 200 mb (not shown) are out of phase with these 850-mb anomalies, as is consistent with the structure of equatorial Kelvin/Rossby waves associated with the MJO.

Enhanced convection in the eastern Pacific Ocean is associated with strong 850-mb westerly wind anomalies at phase 2. These westerly anomalies propagated eastward from the western Pacific Ocean and are associated with the previous cycle of MJO convection. Initiation of the westerly wind anomalies occurs near and to the west of western Pacific convection during phases 6 and 8. These anomalies then propagate into the eastern Pacific and amplify by phase 9 (not shown). Although the MJO is not perfectly periodic, phase 9 composites are very similar to phase 1 (not shown). The westerly wind anomalies then achieve their peak magnitude over the eastern Pacific at phase 2. The propagation of these westerly anomalies into the eastern Pacific is also consistent with Kelvin wave dynamics. The wind anomalies are locally amplified over the eastern Pacific through interactions with convection. Topographic forcing of convection over Central America may be a factor.

To confirm the eastward propagation of wind anomalies from the western Pacific into the eastern Pacific, lag correlations between the averaged equatorial (10°N–10°S) 850-mb zonal wind time series at 102.5°W and all other equatorial longitudes are displayed in Fig. 4. The zonal wind time series was bandpass-filtered to 20–80 days to concentrate on intraseasonal variability and uses data from May to November 1979–95. Shading represents where correlations are significant at the 95% level. Eastward propagation of intraseasonal zonal wind signals is evident from the western Pacific into the eastern Pacific. Zonal winds in the eastern Pacific lag those near 100°E by about 15 days. An out-of-phase relationship occurs between zonal winds in the eastern Pacific and those west of 150°E at zero lag. The eastward movement of the zonal wind signal increases to the east of 180°, a fact confirmed by previous studies (e.g., Hendon and Salby 1994).

4. Eastern Pacific composites

Phases 2 and 6 represent the periods of peak westerly and easterly 850-mb equatorial wind anomalies over the eastern Pacific during the MJO life cycle. They also correspond to the times of peak enhanced and suppressed convection. This section will focus on these two phases in the context of the eastern Pacific hurricane region. Particular emphasis will be placed on the fields of low-level vorticity and vertical wind shear, since these are the two most important time-variant environmental variables for tropical cyclone development (Gray 1979; McBride and Zehr 1981).

Figure 5 displays 850-mb wind anomalies and 850-mb relative vorticity anomalies at phases 2 and 6 for the regions 150°–60°W, 20°S–40°N. Strong westerly wind anomalies at 850 mb are present to the north of the equator during phase 2. The westerly anomalies are locally amplified by enhanced convection. The westerly

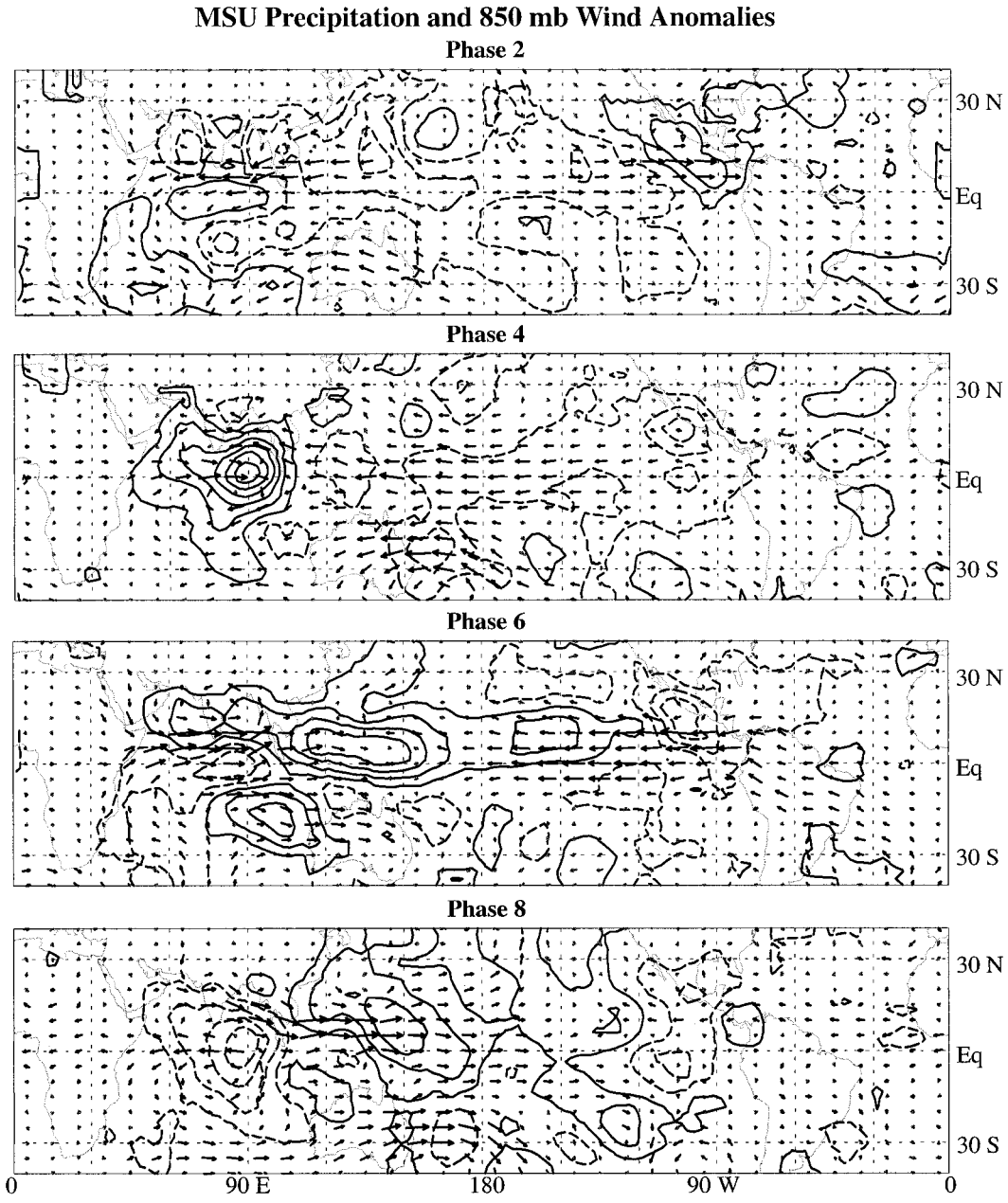

FIG. 3. Composites of bandpassed 850-mb wind anomalies and MSU precipitation anomalies during May–Nov 1979–95 for phases 2, 4, 6, and 8. Maximum vectors are 3.0 m s^{-1}. Precipitation contours are at intervals of 0.6 mm day^{-1} starting at 0.3 mm day^{-1}. Negative contours are dashed. Precipitation values are smoothed spatially using a 1–2–1 filter. The precipitation product is only valid over ocean areas.

wind anomalies may be further enhanced by tropical cyclone growth and associated latent heat release. Strong cyclonic relative vorticity anomalies ($\sim 0.5 \times 10^{-5}$ s^{-1}) lie just to the north of the strongest wind anomalies. These strong vorticity anomalies, due mainly to meridional shear of the zonal wind, are coincident with positive precipitation anomalies (Fig. 6). Precipitation anomalies in Fig. 6 are plotted at higher resolution than those in Fig. 3. The unfiltered vorticity field (not bandpass filtered, not shown) is strongly cyclonic at this time. Low-level wind anomalies during phase 2 may be creating a favorable environment for tropical cyclone formation because of instabilities caused by cyclonic meridional shear of the zonal wind (Gray 1979; Schubert et al. 1991; Molinari et al. 1997; Nieto Ferreira and Schubert 1997). Cyclonic shear, through interactions with the boundary layer, can also foster low-level convergence and upward motion, conditions that are fa-

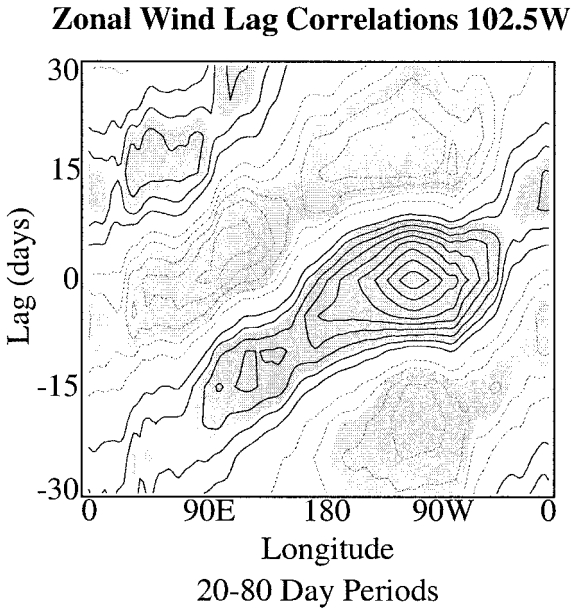

FIG. 4. Lag correlations of the 850-mb zonal wind averaged from 10°N to 10°S as a function of longitude. The reference time series is at 102.5°W. Winds were bandpass-filtered to 20–80 days. May–Nov data during 1979–95 were used. Contours are every 0.1 with negative correlations dashed. Shading indicates where correlations are significantly different from zero at the 95% level.

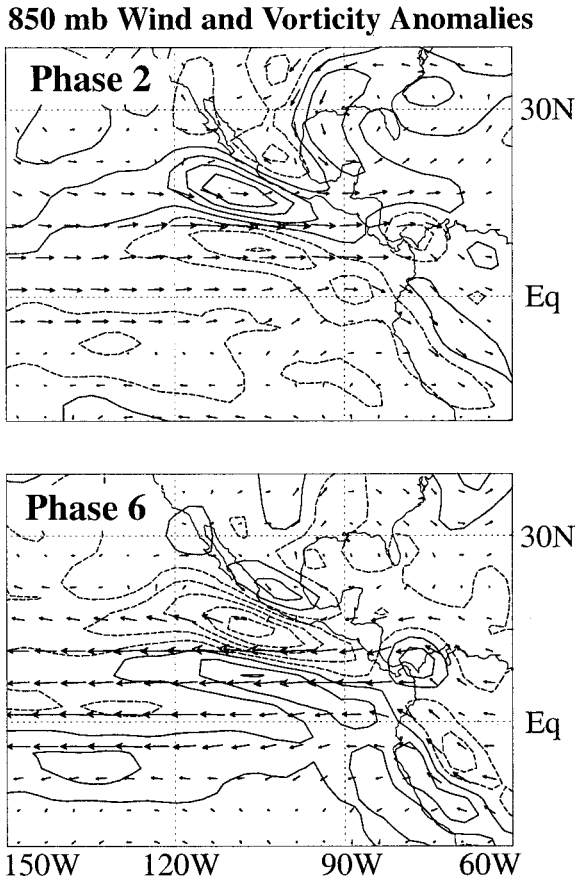

FIG. 5. The 850-mb bandpassed wind anomalies and 850-mb relative vorticity anomalies during May–Nov 1979–95 for phases 2 and 6. Maximum vectors are 3.0 m s^{-1}. Contours are every 1.2×10^{-6} s^{-1} starting at 0.6×10^{-6} s^{-1}. Negative contours are dashed.

vorable for tropical cyclone growth. The situation in the eastern Pacific may be similar to tropical cyclone formation during periods of westerly winds in the western Pacific Ocean (Nitta 1989; Hartmann et al. 1992; Liebmann et al. 1994; Nieto Ferreira et al. 1996). Strong easterly 850-mb wind anomalies occur during phase 6. Strong anticyclonic vorticity anomalies ($\sim -0.5 \times 10^{-5}$ s^{-1}) are located in the hurricane region just to the north of the maximum wind anomalies and coincide with suppressed convection (Fig. 6). The unfiltered relative vorticity field (not shown) is also anticyclonic at phase 6. Some of the strongest 850-mb wind anomalies in the global composites occur in this region during phase 6.

The difference between 850-mb relative vorticity anomalies at phases 2 and 6 is plotted in Fig. 7. Differences greater than 1.0×10^{-5} s^{-1} can be found over the eastern Pacific hurricane genesis region. A comparison with the results of McBride and Zehr (1981) indicates that these differences are similar to those seen between environments supporting developing tropical systems and environments in which tropical systems do not develop. Low-level vorticity differences of 0.4×10^{-5} s^{-1} were seen in their composites between periods in which strong developing systems existed and periods in which only weak developing systems existed. Therefore, the low-level relative vorticity changes between phases 2 and 6 are significant in the context of tropical cyclone development. Tropical cyclones may magnify the vorticity anomalies through latent heat release and associated circulation intensification. However, since the location and sign of relative vorticity anomalies during phases 2 and 6 are consistent with MJO Kelvin wave dynamics, the MJO is likely the primary driver behind these anomalies and amplification of the wave circulation likely occurs through interactions with convection not organized into tropical cyclones.

Figure 8 displays 200-mb wind anomalies and 200-mb vorticity anomalies. Easterly (westerly) 200-mb equatorial wind anomalies occur at phase 2 (phase 6). The strongest wind anomalies at 200 mb during both phases occur to the south of the equator. Vorticity anomalies associated with these wind anomalies show anticyclonic (cyclonic) vorticity at 200 mb centered well to the south of enhanced (suppressed) convection centers (see Fig. 6). Other vorticity centers occur to the north of the hurricane region. However, *mean* 200-mb vorticity is highly anticyclonic over the eastern Pacific hurricane genesis region. Upper-level wind anomalies alter these values little. Low-level vorticity anomalies seem to be more important than upper-level anomalies for cyclone development in the context of an MJO life cycle. Upper-level wind anomalies, however, may contribute to vertical shear variations.

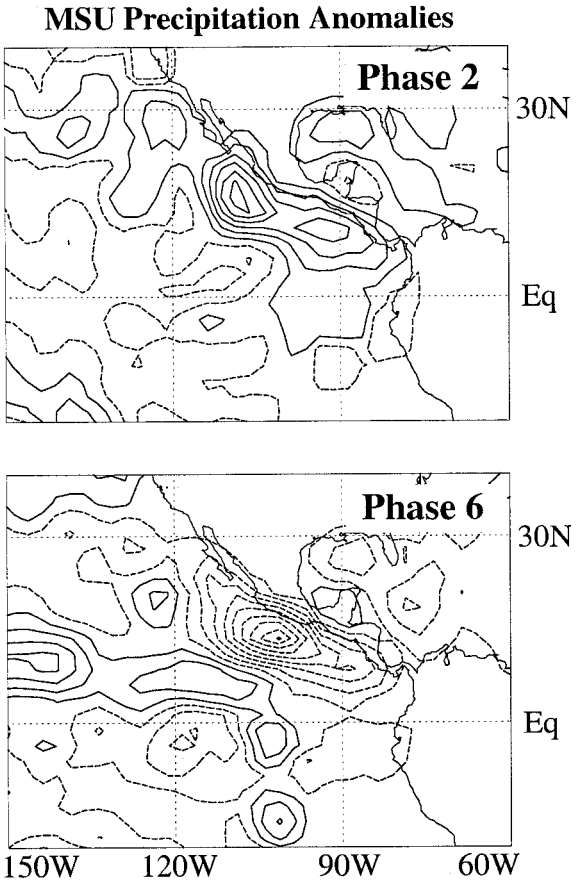

FIG. 6. MSU precipitation anomalies during May–Nov 1979–95 for phases 2 and 6. Contours are every 0.6 mm day^{-1} starting at 0.3 mm day^{-1}. Negative contours are dashed. No smoothing is used. The precipitation product is valid only over ocean areas.

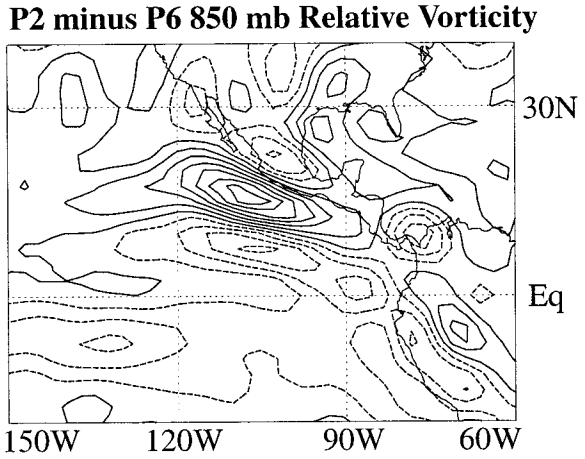

FIG. 7. The difference between 850-mb relative vorticity anomalies at phases 2 and 6 (phase 2 minus phase 6), during May–Nov 1979–95. Contours are every 1.6 $\times$ 10^{-6} s^{-1} starting at 0.8 $\times$ 10^{-6} s^{-1}. Negative contours are dashed.

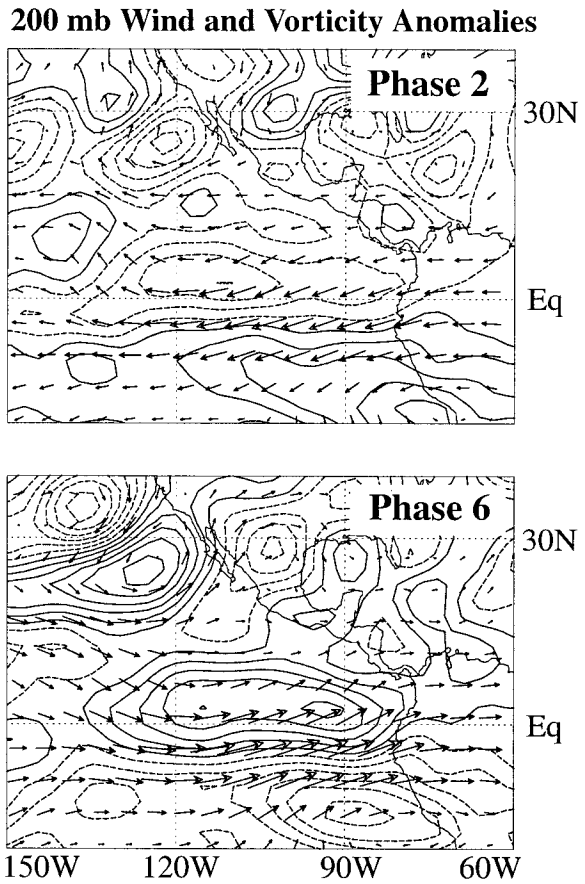

FIG. 8. Bandpassed 200-mb wind and 200-mb relative vorticity anomalies during May–Nov 1979–95 for phases 2 and 6. Maximum vectors are 7.0 m s^{-1}. Contours are every 1.2 $\times$ 10^{-6} s^{-1} starting at 0.6 $\times$ 10^{-6} s^{-1}. Negative contours are dashed.

Tropical cyclones tend to form near areas of zero vertical shear of the zonal wind between strong positive vertical shear of the zonal wind to the north and strong negative vertical shear of the zonal wind to the south (Gray 1968; McBride and Zehr 1981; Elsberry et al. 1988). Positive shear is defined as upper-level winds being more westerly than lower-level winds. Tropical cyclogenesis is favored near regions of zero shear because higher vertical shears would tend to tilt the vortex circulation in the vertical. This vertical tilting leads to an increased midlevel temperature perturbation and suppression of convection (DeMaria 1996). Figure 9 shows the unfiltered vertical wind shear between the 200- and 850-mb levels for phases 2 and 6. Only the zonal wind is used in the vertical shear computations since the shear of the meridional wind in the composites is insignificant. The zero shear line lies over the hurricane genesis region during phase 2 with strong negative shear to the south and strong positive shear to the north. The zero shear line lies to the south of the hurricane genesis region during phase 6. The magnitude of positive (negative) vertical shear to the north (south) of the zero line is smaller during phase 6 than phase 2. Thus, wind anom-

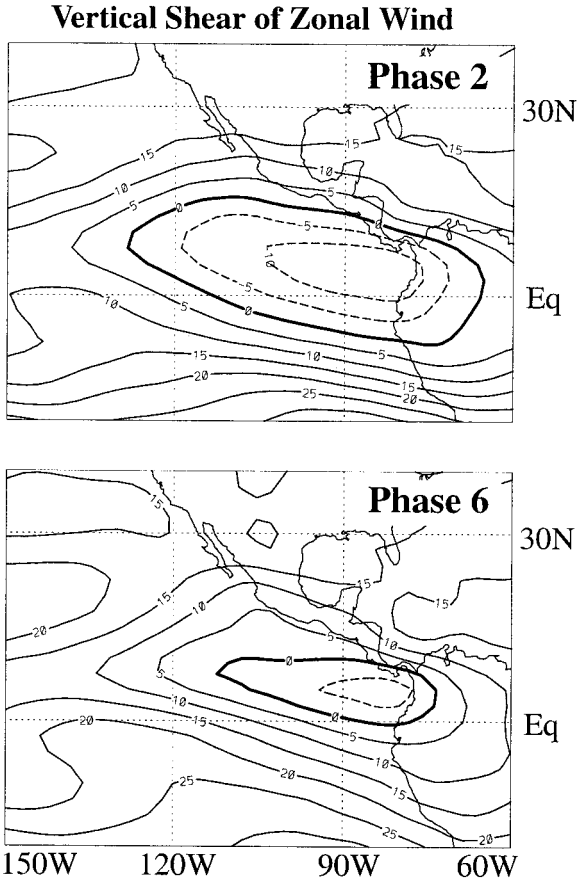

FIG. 9. The 200-mb zonal wind minus 850-mb zonal wind during May–Nov 1979–95 for phases 2 and 6. Values are not anomalies but total shear values. Contours are every 5.0 m s^{-1} starting at 0.0 m s^{-1}. Negative contours are dashed. Positive values mean that 200-mb winds are more westerly than 850-mb winds.

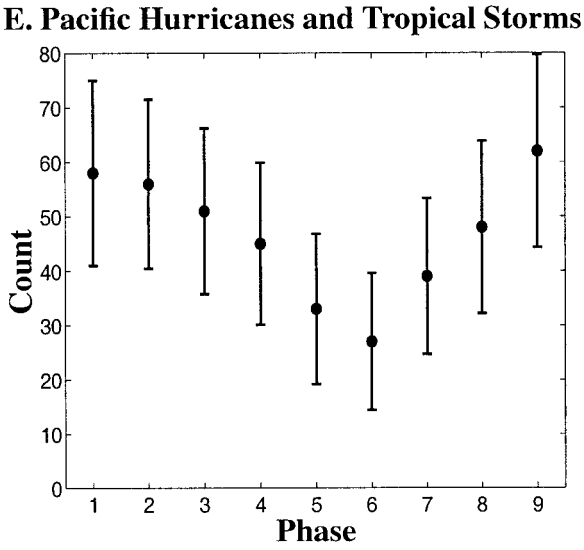

FIG. 10. Number of hurricanes and tropical storms as a function of MJO phase for the eastern Pacific Ocean hurricane region during May–Nov 1979–95. Error bars represent 95% confidence limits.

alies associated with the MJO would tend to create a vertical wind shear profile favorable for tropical cyclone development during phase 2 and one less favorable during phase 6.

In summary, the MJO composites show more favorable low-level vorticity and vertical wind shear profiles for eastern Pacific hurricane development during 850-mb equatorial westerly anomalies (phase 2) than during 850-mb equatorial easterly anomalies (phase 6). These environmental conditions coincide with enhanced phase-2 convection and suppressed phase-6 convection. Actual records of eastern Pacific hurricanes and tropical storms must now be examined to confirm that the MJO modulates eastern Pacific tropical systems.

5. Tropical cyclone composites

Figure 10 displays the number of named systems in the eastern Pacific hurricane region (east of 140°W) occurring during each phase of the MJO for May–November 1979–95. Results do not differ significantly when using data from June to September, the period of peak hurricane activity. The *t* statistic was used to determine 95% confidence limits. Named systems include tropical storms (winds $\geq$ 34 kt) and hurricanes (winds $\geq$ 64 kt). A particular tropical system may span more than one phase and therefore can be added to the count of more than one phase. A discernible cycle in the number of named systems is observed as one progresses from phase 1 to phase 9. Over twice the number of named tropical systems exist in both phase 1 and phase 2 than in phase 6. Phase 2 has 56 named tropical systems as opposed to 27 in phase 6. An identical analysis using genesis events (i.e., the times at which systems attain a wind speed of 34 kt) produces a similar result (not shown).

The average strength of tropical storms and hurricanes as a function of phase is plotted in Fig. 11 along with confidence limits. The strength of a particular tropical system in a phase category is defined as the strongest sustained wind speed (kt) recorded in association with that system during that phase. The same system can contribute different strengths in two different phase categories. A pronounced cycle is again seen during the progression through the phases. Average system strength at phase 2 is 88 kt as opposed to 67 kt at phase 6. Figures 10 and 11 indicate that fewer named tropical systems exist in phase 6 (equatorial 850-mb easterlies) than in phase 2 (equatorial 850-mb westerlies), and the ones that do exist are weaker. These facts would suggest that hurricanes are more likely during phase 2 than during phase 6.

Figure 12 plots the number of hurricanes as a function of phase along with confidence limits. Over four times as many hurricanes are present during phase 2 than during phase 6 (44 vs 10). Precipitation anomalies seen in the composite life cycle over the eastern Pacific do in-

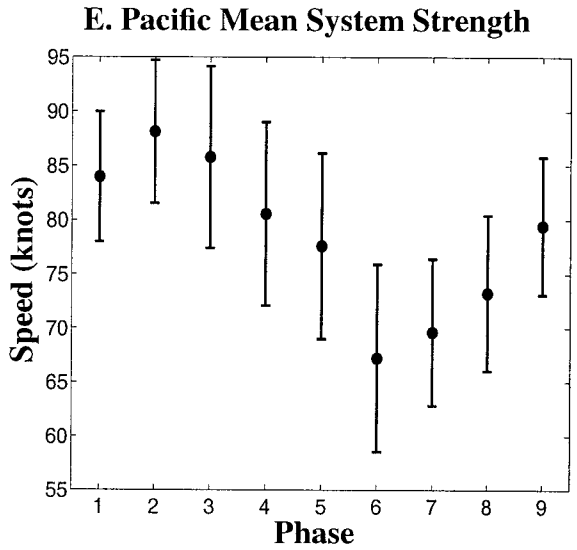

FIG. 11. Average strength (kt) of hurricanes and tropical storms as a function of MJO phase for the eastern Pacific Ocean hurricane region during May–Nov 1979–95. Error bars represent 95% confidence limits.

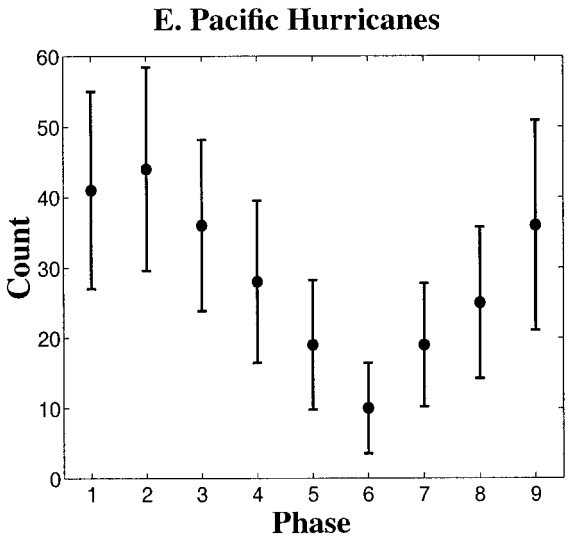

FIG. 12. Number of hurricanes as a function of MJO phase for the eastern Pacific Ocean hurricane region during May–Nov 1979–95. Error bars represent 95% confidence limits.

deed coincide with a modulation of the number and strength of tropical systems. This statistically robust result indicates that the MJO significantly alters environmental conditions over its life cycle to modulate hurricane activity in the eastern Pacific.

6. Conclusions

A pronounced cycle in the number of named tropical systems in the eastern Pacific Ocean occurs during a composite life cycle of the Madden–Julian oscillation. Periods of westerly equatorial 850-mb wind anomalies over the eastern Pacific account for twice as many hurricanes and tropical storms as do periods of easterly anomalies. Average system strength is also significantly affected. Hurricanes in westerly periods outnumber those in easterly periods by more than four to one.

The modulation of hurricane activity over an MJO life cycle can be attributed to changes in environmental conditions in the eastern Pacific. MJO Kelvin waves may influence the large-scale environment over the eastern Pacific hurricane region. Kelvin waves that propagate eastward from western Pacific convective areas enhance convection over the eastern Pacific. Zonal wind anomalies associated with the MJO wave are locally amplified by this anomalous convection. Rossby waves forced by convection and convective inflow over Central America may contribute to the strength of eastern Pacific wind anomalies. Topographic forcing of convection over Central America may be a factor. Low-level relative vorticity and vertical wind shear are important environmental dynamic variables associated with tropical cyclone formation. Periods of 850-mb westerly equatorial wind anomalies over the eastern Pacific are characterized by anomalously high 850-mb relative vorticity and a zero line in vertical wind shear near the hurricane genesis region, which are conditions favorable for cyclone development. Easterly wind periods coincide with anomalously anticyclonic 850-mb relative vorticity and a less favorable vertical shear profile, which are conditions detrimental to cyclone development. Upper-level vorticity anomalies do not seem to play a consistent role in altering environmental conditions over the eastern Pacific during an MJO life cycle since they are not collocated with the hurricane genesis region. Upper-level mean vorticity, however, is highly anticyclonic during the eastern Pacific hurricane season. Since the MJO is weakest in Northern Hemisphere summer, it is likely that not all tropical cyclones in the eastern Pacific are affected by the MJO. The results of this paper suggest that MJO events can significantly modulate hurricane activity over this region, however.

Westerly wind bursts in the western Pacific have a tendency to support tropical cyclone formation because of strong cyclonic shear on the flanks of the equatorial wind anomalies. A similar process might be occurring over the eastern Pacific during certain phases of the MJO. Cyclone intensification can then reinforce wind anomalies toward the equator, creating a positive feedback. In fact, some of the strongest wind anomalies in the global MJO composites occur in the eastern Pacific Ocean region. Convection not associated with tropical cyclones, however, may be a more important factor in strengthening eastern Pacific wind anomalies.

Future work might be needed to address the contribution of cyclogenesis to strengthening the wind anomalies in the eastern Pacific at upper and lower levels. Convection over the eastern Pacific, Mexico, Central America, and the Caribbean strengthens eastward-prop-

agating wind anomalies over the eastern Pacific Ocean. The contributions of the signal that come from enhancement by undeveloped convection and from tropical cyclone enhancement need to be separated if possible. A modeling study addressing the effects of tropical cyclone latent heating and vortex spinup on zonal wind distributions and shear zones might be enlightening. Such work would be relevant for other hurricane regions such as the western Pacific as well. Regardless, zonal wind anomalies associated with Kelvin wave propagation from the west would appear to be the principal driver in altering environmental conditions for cyclogenesis in the eastern Pacific during a MJO life cycle.

Acknowledgments. The authors would like to thank the NOAA NWS Tropical Prediction Center for use of hurricane and tropical storm tracking data. Two anonymous reviewers provided helpful insight on the manuscript. This work was supported by the Climate Dynamics Program of the National Science Foundation under Grant ATM-9313383.

REFERENCES

Brown, G. M., and P. W. Leftwich Jr., 1982: A compilation of eastern and central North Pacific tropical cyclone data. NOAA Tech. Memo. NWS NHC 16, 15 pp.

Charney, J. G., and M. E. Stern, 1962: On the stability of internal baroclinic jets in a rotating atmosphere. *J. Atmos. Sci.*, **19,** 159–172.

Davidson, N. E., G. J. Holland, J. L. McBride, and T. D. Keenan, 1990: On the formation of AMEX Tropical Cyclones Irma and Jason. *Mon. Wea. Rev.*, **118,** 1981–2000.

DeMaria, M., 1996: The effect of vertical shear on tropical cyclone intensity change. *J. Atmos. Sci.*, **53,** 2076–2087.

Elsberry, R. L., E. L. Weniger, and D. H. Meanor, 1988: A statistical tropical cyclone intensity forecast technique incorporating environmental wind and vertical wind shear information. *Mon. Wea. Rev.*, **116,** 2142–2154.

Gray, W. M., 1968: Global view of the origin of tropical disturbances and storms. *Mon. Wea. Rev.*, **96,** 669–700.

——, 1979: Hurricanes: Their formation, structure, and likely role in the tropical circulation. *Meteorology over the Tropical Oceans,* D. B. Shaw, Ed., Royal Meteorological Society, 155–218.

Hartmann, D. L., M. L. Michelsen, and S. A. Klein, 1992: Seasonal variations of tropical intraseasonal oscillations: A 20–25-day oscillation in the western Pacific. *J. Atmos. Sci.*, **49,** 1277–1289.

Hendon, H. H., and M. L. Salby, 1994: The life cycle of the Madden–Julian oscillation. *J. Atmos. Sci.*, **51,** 2225–2237.

Holton, J. R., 1992: *An Introduction to Dynamic Meteorology.* Academic Press, 511 pp.

Kalnay, E., and Coauthors, 1996: The NCEP/NCAR 40-Year Reanalysis Project. *Bull. Amer. Meteor. Soc.*, **77,** 437–471.

Liebmann, B., H. H. Hendon, and J. D. Glick, 1994: The relationship between tropical cyclones of the western Pacific and Indian Oceans and the Madden–Julian oscillation. *J. Meteor. Soc. Japan,* **72,** 401–412.

Madden, R. A., and P. R. Julian, 1994: Observations of the 40–50-day tropical oscillation—A review. *Mon. Wea. Rev.*, **122,** 814–837.

Maloney, E. D., and D. L. Hartmann, 1998: Frictional moisture convergence in a composite life cycle of the Madden–Julian oscillation. *J. Climate,* **11,** 2387–2403.

McBride, J. L., and R. Zehr, 1981: Observational analysis of tropical cyclone formation. Part II: Comparison of nondeveloping versus developing systems. *J. Atmos. Sci.*, **38,** 1132–1151.

Molinari, J., and D. Vollaro, 1989: External influences on hurricane intensity. Part I: Outflow layer eddy angular momentum fluxes. *J. Atmos. Sci.*, **46,** 1093–1105.

——, D. Knight, M. Dickinson, D. Vollaro, and S. Skubis, 1997: Potential vorticity, easterly waves, and eastern Pacific tropical cyclogenesis. *Mon. Wea. Rev.*, **125,** 2699–2708.

Nieto Ferreira, R., and W. H. Schubert, 1997: Barotropic aspects of ITCZ breakdown. *J. Atmos. Sci.*, **54,** 261–285.

——, ——, and J. J. Hack, 1996: Dynamical aspects of twin tropical cyclones associated with the Madden–Julian oscillation. *J. Atmos. Sci.*, **53,** 929–945.

Nitta, T., 1989: Development of a twin cyclone and westerly bursts during the initial phase of the 1986–1987 El Niño. *J. Meteor. Soc. Japan,* **67,** 677–681.

——, and M. Yanai, 1969: A note on the barotropic instability of the tropical easterly current. *J. Meteor. Soc. Japan,* **47,** 127–130.

North, G. R., T. L. Bell, R. F. Cahalan, and F. J. Moeng, 1982: Sampling errors in the estimation of empirical orthogonal functions. *Mon. Wea. Rev.*, **110,** 699–706.

Salby, M. L., and H. H. Hendon, 1994: Intraseasonal behavior of clouds, temperature, and motion in the Tropics. *J. Atmos. Sci.*, **51,** 2220–2237.

Schubert, W. H., P. E. Ciesielski, D. E. Stevens, and H. Kuo, 1991: Potential vorticity modeling of the ITCZ and the Hadley circulation. *J. Atmos. Sci.*, **48,** 1493–1509.

Spencer, R. W., 1993: Global ocean precipitation from the MSU during 1979–91 and comparisons to other climatologies. *J. Climate,* **6,** 1301–1326.

Zehr, R. M., 1992: Tropical cyclogenesis in the western North Pacific. NOAA Tech. Rep. NESDIS 61, 181 pp. [Available from NOAA/NESDIS, 5200 Auth Rd., Washington, DC 20233.]